High-Temperature Photoluminescence of CdSe/CdS Core/Shell Nanoheterostructures

Benjamin T. Diroll[†] and Christopher B. Murray[†,‡,*]

[†]Department of Chemistry and [‡]Department of Materials Science and Engineering, University of Pennsylvania, Philadelphia, Pennsylvania 19104, United States

ABSTRACT The steady-state and time-resolved photoluminescence properties of CdSe/CdS heterostructures are studied as a function of temperature from 300 to 600 K. The emission properties of samples are found to behave similarly to bulk CdSe, with the samples maintaining high color purity and a slightly contracting band gap at elevated temperature. Photoluminescence from CdSe/CdS samples is maintained with high stability over prolonged illumination and multiple heating and cooling cycles. Structures synthesized with variation in the core and the shell dimensions show that the preservation of emission intensity at high temperature depends strongly on the microscopic structure of the samples. For samples synthesized by seeded growth, the size of the CdSe core is highly correlated with the fraction of preserved sample photoluminescence intensity at high temperature. Temperature-dependent lifetime data suggest that the core structure predicts the stability of photoluminescence at elevated temperatures by controlling the radiative rate. The rate of electron capture, for which the volume fraction of the core is a structural proxy, underpins the ability for radiative processes to compete with thermally induced nonradiative decay pathways. Heterostructures synthesized below 200 °C using highly reactive organometallic precursors show markedly lower thermal stability than samples prepared by seeded growth at 360 °C, suggesting that the temperature of nanocrystal synthesis has direct consequences for the thermal stability of photoluminescence.

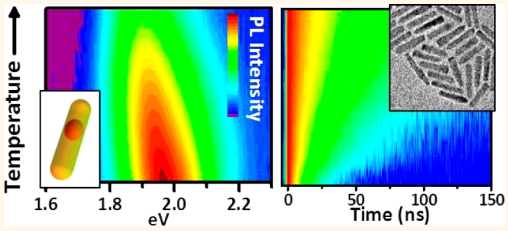

KEYWORDS: photoluminescence · thermal stability · colloidal nanomaterials · time-resolved photoluminescence

Temperature-dependent studies of semiconductor nanocrystal (NC) emission properties above room temperature represent an emerging area of interest as research into NC-based devices moves toward technological implementation.[1−10] Functioning devices, such as photovoltaics,[11,12] LEDs,[13,14] color converting layers,[15] luminescent concentrators,[16,17] and NC-based lasers[18] may require stable, high-performance operation at elevated temperatures. Displays in particular require phosphors with sustained brightness and high color purity at temperatures frequently exceeding 100 °C. Temperature-dependent optical studies of colloidal semiconductor NCs are commonly performed at low temperature to elucidate electronic and excitonic structure in the absence of thermal broadening.[19,20] Studies of the evolution of photoluminescence (PL) at temperatures closer to the operating range of optoelectronic devices remain limited. There is relatively little understanding of how synthetically controllable parameters—size, shape, composition, electronic structure—contribute to the stability or instability of PL at temperatures exceeding 300 K. The study of these variables has the potential to contribute to improvements in device performance.

In this context, seeded-growth CdSe/CdS nanorods (NRs) are excellent candidates for light-emitting applications and study at high temperature. The presence of an anisotropic CdS shell yields samples that combine high PL quantum yields, excellent color purity, and strongly polarized emission.[21−23] Similar to spherical core/shell systems, samples can be prepared with many core sizes and shell thicknesses. In contrast to spherical core/shell systems, CdSe/CdS NRs allow a separate treatment of the shell thickness in the short axis and the total heterostructure size. Earlier works on II−VI[2−4] and III−V NCs[1] have shown that core/shell NCs show improved thermal stability of PL in terms of preserved luminescence and reversibility of PL loss. In this work, we examine PL properties of a family of CdSe/CdS nanoheterostructures prepared by seeded growth to investigate

* Address correspondence to cbmurray@sas.upenn.edu.

Received for review April 17, 2014 and accepted May 13, 2014.

Published online May 13, 2014
10.1021/nn5021314

how NC core and shell dimensions contribute to PL behavior from 300 to 600 K. We found that the degree to which PL is preserved at high temperature in CdSe/CdS core/shell NRs depends on the physical dimensions of the core/shell NR and the method of sample preparation. Thermal cycling experiments suggest that PL quenching occurs primarily through thermally reversible formation of single carrier trap sites consistent with previous reports.[2,4] Time-resolved PL experiments suggest that samples with faster radiative decay—determined by the physical size of the core and the shell components—show less PL quenching at elevated temperature.

RESULTS AND DISCUSSION

Thermal Stability of Photoluminescence from Seeded Growth Heterostructures. Figure 1 shows the typical optical and structural properties of CdSe/CdS dot-in-rod NCs. Spherical CdSe NCs with wurtzite structure (Figure 1a) are reacted at 350−360 °C in a seeded growth synthesis to grow a heteroepitaxial CdS shell that forms an elongated NR (Figure 1b). The product dot-in-rod heterostructures show a red-shift of the first excitonic absorption feature (Figure 1c), similar to results for isotropically overcoated CdSe NCs.[24] The addition of the large CdS shell results in substantially increased absorption for energies greater than 2.5 eV. Structurally, the wurtzite CdSe NCs, with broad X-ray scattering features, transform into a CdS rod, with the anisotropic growth particularly evident in the sharpness of the [002] reflection at 27.5° (Figure 1d).

In this study we employ samples in which the core size and heterostructure dimensions are tuned to investigate patterns in the PL behavior at high temperatures. In contrast to some previous studies, in which temperature-dependent emission was studied to 800 K,[1,2] limiting the highest temperature to 600 K ensures that the NCs do not sinter and even maintain solution dispersibility. Figure S1 shows the CdSe NR sample before heating and the same sample after heating and cooling followed by quantitative redispersion in hexanes. After gentle agitation from stirring, nearly all NRs were liberated from the substrate surface. Absorption and emission curves of the sample before and after heating are superimposable, despite strongly quenched PL at 600 K. This represents the strongest evidence that the structure of the NCs remains intact throughout the experiment and the results are not affected by irreversible structural changes such as sintering or phase transitions.

Figure 2a−d show contour plots of the temperature-dependent emission from four samples of dot-in-rod NCs in which the CdSe core sizes used in seeded growth are 2.2 nm "small" NCs, 3.8 × 3.6 nm "medium" NCs, prolate 6.8 × 5.8 nm "large" NCs, and 12.8 nm × 4.3 nm CdSe NRs. In each case, the fluorescence intensity (with 405 nm excitation) decreases with

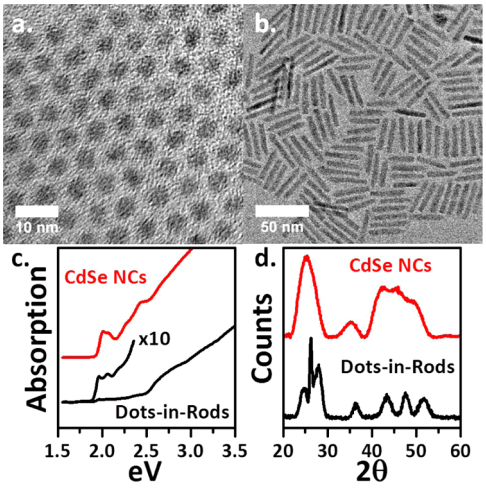

Figure 1. TEM images of (a) CdSe NCs and (b) CdSe/CdS dot-in-rod heterostructures. (c) Absorption measurements of both CdSe NCs and a sample of dots-in-rods made by seeded growth using the same NC sample. (d) X-ray patterns of CdSe NCs offset *versus* that of a CdSe/CdS dot-in-rod sample.

temperature elevation. At the same time, the fluorescence broadens and red-shifts. The positions of the emission maxima and the full-widths at half-maximum (fwhm) were determined by fitting each emission profile to a Gaussian peak. The results for these four samples are plotted in Figure 2e and f. Similar to earlier reports,[8,25] the emission maximum shifts from the band gap at 0 K ($E_{gap}(0)$) in reasonable agreement with the Varshni relation,[26] approximating a linear change at high temperature:

$$E_{gap}(T) = E_{gap}(0) - \alpha T^2/(\beta + T) \quad (1)$$

Using the values of $\alpha = 2.7 \times 10^{-4}$, the temperature coefficient, and $\beta = 195$ K, approximating the Debye temperature,[8] we find a reasonable fit to the data collected on dot-in-rod and rod-in-rod samples studied in this work that is consistent with the literature[6−8,25] (Supporting Information Figure S2).

The PL broadening shown in Figure 2f indicates that the color purity of core/shell NCs decreases at elevated temperature, but this result is also in relatively good agreement with the predicted broadening of fluorescence that has been found in CdSe/ZnS[8] and CdSe/CdS[25] NCs. PL broadening follows a function

$$\Gamma(T) = \Gamma_{inh} + \Gamma_{AC}T + \Gamma_{LO}(e^{E_{LO}/kT} - 1)^{-1} \quad (2)$$

in which Γ_{inh} is the intrinsic inhomogeneous line width, Γ_{AC} is the acoustic phonon−exciton coupling coefficient, Γ_{LO} is the longitudinal optical (LO) phonon−exciton coupling coefficient, and E_{LO} is the LO phonon energy. The experimental change in broadening is plotted for every dot-in-rod and rod-in-rod sample measured in this study in Figure S2 along with a line based on the literature ($\Gamma_{inh} \approx 40$ meV; $\Gamma_{AC} \approx 55\ \mu$eV/K; $\Gamma_{LO} \approx 20$ meV; $E_{LO} \approx 30$ meV).[3,25] The PL properties of

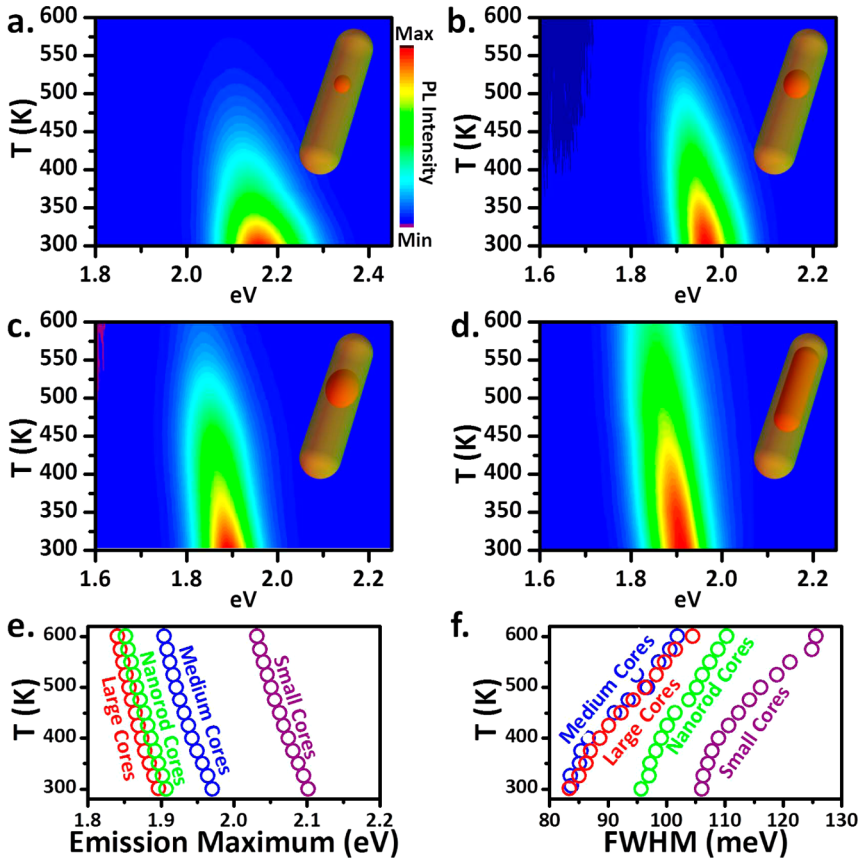

Figure 2. (a–d) Normalized contour plots of the temperature-dependent emission from CdSe/CdS dot-in-rod heterostructures with cartoons of the samples overlaid on the plot. Temperature-dependence of the emission energy of maximum intensity (e) and full-width at half-maximum (fwhm) (f) for the same four samples.

the samples studied in this work behave similarly to bulk CdSe and other NCs studied at lower temperature in terms of both the temperature-dependent band gap and homogeneous emission broadening.

The temperature-dependent PL intensity is plotted for several samples in Figure 3, with the values normalized to the initial intensity at 300 K. Figure 3a shows the integrated intensity data collected from heating the four NR samples shown in Figure 2. (Cooling data for the same samples can be found in Supporting Information Figure S3.) The samples plotted in Figure 3a show substantial differences in the quantity of PL quenching at 600 K. PL quenching of the small core sample is greater (to ~1.5% of the original intensity at 600 K) than those made with the larger cores. The degree of quenching appears to be directly related to the heterostructure core.

More finely controlled structure–property relationships are tested by tuning the shell thickness separately in the transverse and longitudinal directions. For Figure 3b, small CdSe cores were used to synthesize three samples with very similar length (30 nm) but in which the shell thickness was varied substantially from 1.1 to 1.5 nm. Increasing shell thickness is correlated with less blinking[27] and higher PL quantum yields. In these measurements, thicker shells confer enhanced thermal stability of PL, but this effect is far less substantial than changes of the heterostructure volume. For Figure 3c, large CdSe cores were used to synthesize samples with fixed shell thickness, but the NR lengths varied between 25 and 78 nm to study the role of heterostructure volume on the thermal stability of PL. Similar to the trend apparent in Figure 3a, Figure 3c highlights the evidence that those CdSe/CdS samples in which the core comprises a larger volume fraction of the total heterostructure are more resistant to PL quenching. Further confirmation of this trend comes from the synthesis of isotropic CdSe/CdS heterostructures with a slightly modified procedure using oleic acid rather than phosphonic acids as the dominant ligand.[28] Among these samples, PL is most strongly preserved in the sample with the thinnest shell but the largest CdSe core volume fraction (Supporting Information Figure S4). Although core/shell samples enhanced thermal stability of PL compared to core-only samples (Figure S1), within the series of core/shell samples tested in this study, room-temperature quantum yield is not a good indicator of thermally stable PL (Supporting Information Figure S5).

In addition to the temperature-dependent data taken by heating and cooling samples to and from 600 K, we also tested the cycling and medium-term

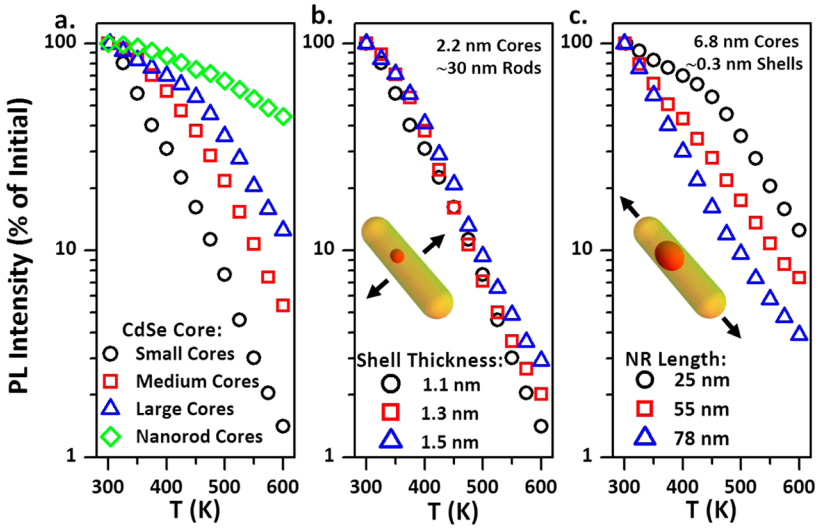

Figure 3. (a) Integrated, normalized PL intensity plotted *versus* temperature for three samples of dot-in-rod CdSe/CdS NCs and one rod-in-rod NC. (b, c) Relative PL intensity plotted *versus* temperature for dot-in-rod samples in which the shell thickness (b) or the NR length (c) is varied.

stability of a CdSe/CdS NR sample at moderate temperature (140 °C, 412 K), comparable to operating temperatures in light-emitting applications. The NRs for this experiment were diluted into a matrix of polyvinylbutyral to model the conditions of operation as phosphors. More common acrylic copolymers formed through radical polymerization were specifically avoided due to PL quenching from radical initiators.[29] This could be the explanation between the apparent discrepancy of the temperature cycling results presented here (and Figure S3) and past work showing poorer reversibility of PL in CdSe/CdS dot-in-rod samples.[4] We tested two measures of stability: cycling between 310 and 412 K (five cycles), shown in Figure 4a, and PL intensity under continuous illumination for 50 000 s, shown in Figure 4b. The sample showed little change in the PL intensity based on the cycle number, consistent with previous proposals that PL quenching is thermally activated but reversible.[2,4] Continuous illumination showed a stable PL signal at long times, but the sample showed photobrightening of ~35% in the first 100 min. Photobrightening in NCs is well known, and much larger magnitudes have been reported,[30] but higher initial quantum yields may place a ceiling on photobrightening. Typically attributed to trap filling, in this case most likely by electrons,[31] the photobrightening behavior can be modeled by an exponential increase following $I_\infty - A\, e^{-t/\tau}$ with a time constant τ of 640 s (Supporting Information Figure S6).[32]

Time-Resolved Photoluminescence of CdSe/CdS Heterostructures. Figure 5 shows time-resolved PL data collected from several samples as a function of temperature. Figure 5a shows the typical relationship of the temperature-dependent lifetime of nanostructures that has been recorded for II–VI NCs: with increasing temperature, nonradiative decay trapping processes dominate over radiative relaxation of excitons and lead

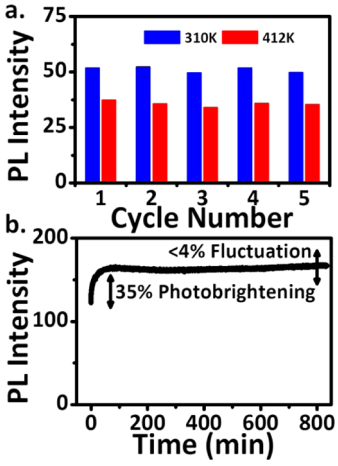

Figure 4. (a) PL intensity of a CdSe/CdS rod-in-rod sample that was heated from 310 K to 412 K in five cycles. (b) Emission intensity of the rod-in-rod sample measured as a function of time at 412 K.

to shorter apparent PL decays.[2,4,33] At higher temperatures, CdSe samples (without a shell) exhibited decays only slightly longer than the instrument response function (Figure 5a and Figure S1). Rowland and Schaller have demonstrated that thermally induced hole trapping, as opposed to intrinsic multiphonon exciton deactivation, explains the decrease in PL and PL lifetime of CdSe and CdSe/ZnS NCs.[2] The addition of a CdS shell leads to substantially different decay behavior for dot-in-rod and rod-in-rod samples shown in Figure 5b and c. In Figure 5b, the dot-in-rod sample shows two trends: slightly increasing decay time to 450 K followed by slightly decreasing decay time. Figure 5c shows the lifetime of the rod-in-rod structure, which exhibits a monotonic increase in PL decay time to 600 K.

Increasing lifetime from 25 K to 300 K has been observed previously in CdSe/CdS NR heterostructures.[25]

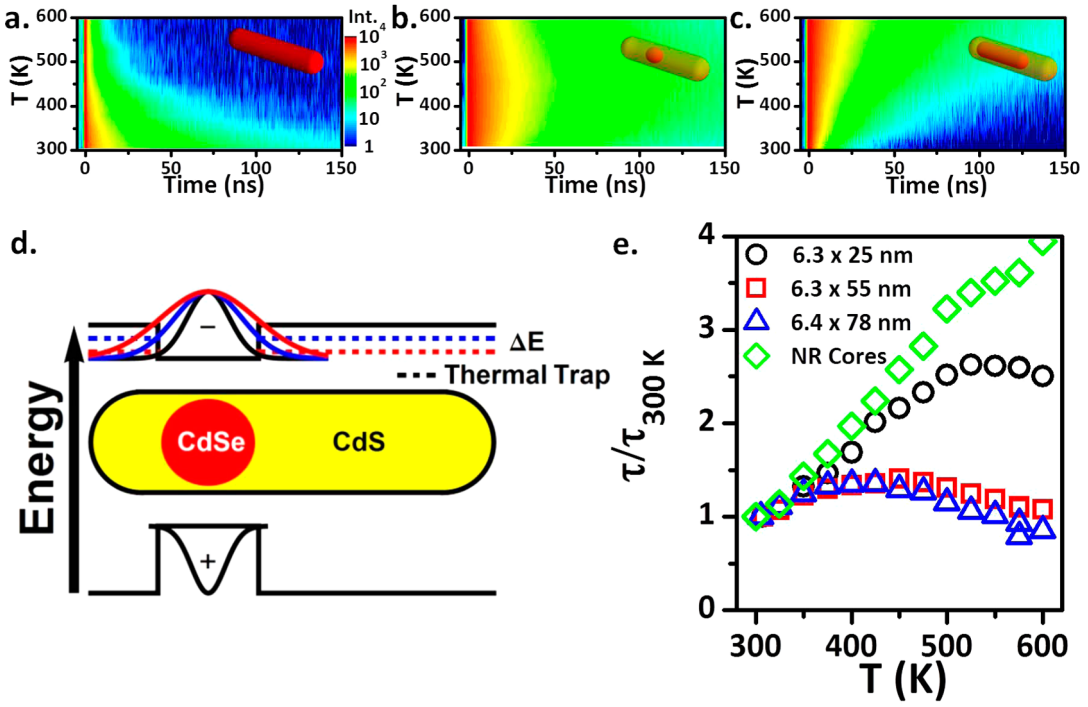

Figure 5. (a–c) Contour plots of time-resolved PL intensity *versus* temperature for samples of CdSe NRs (a), CdSe/CdS dots-in-rods (b), and CdSe/CdS rods-in-rods (c). (d) Cartoon of the band-edge energy states of CdSe/CdS dot-in-rod samples showing the change in the conduction band offset and increased delocalization of the electron at elevated temperatures, symbolized by the blue and red curves. (e) Plot of the PL lifetimes for four CdSe/CdS NR samples made by seeded growth normalized to the lifetime at 300 K.

Figure 5d summarizes the underlying electronic structures of CdSe/CdS heterostructures that explains this phenomenon. Due to band offset and effective mass differences, holes are strongly confined in the CdSe core, but electrons are more freely delocalized into the CdS shell.[25,34−37] The core (hole) and shell (electron) provide an approximation of the excitonic electron and hole wave functions, the overlap of which determines the radiative rate. Due to its greater delocalization, electron capture in the core limits the radiative rate. Thus, samples in which the core material constitutes a larger volume fraction of the total heterostructure show shorter PL lifetimes, although the absolute value may also be altered by such factors as the different band offsets of different core materials, sample history, and the ligand shell (Figure S7). Raino *et al.* found that different temperature-dependent changes in the conduction and valence band energies of CdSe and CdS are responsible for greater electron delocalization at elevated temperatures. As the temperature increases, the conduction band offset of CdSe and CdS decreases slightly, leading to more electron delocalization, smaller electron−hole overlap, and longer radiative lifetimes.[25] Figure 5d models the conduction band change with temperature: at higher temperature, the conduction band offset between the CdSe and CdS decreases, allowing the electron to delocalize more freely, thereby decreasing electron−hole overlap and increasing the radiative lifetime.

Unlike previous temperature-dependent studies up to 300 K,[25] PL of the samples studied in this work decreased at higher temperature. The effects of increasing radiative decay time due to changes in the band offset are convoluted with nonradiative decay. To explain PL quenching, earlier publications have used the concept of thermally generated trap states.[2,4] Intrinsic multiphonon exciton deactivation is unlikely given the large band gap of the CdSe/CdS structures, and this mechanism should yield similar results in all samples. The high reversibility of PL intensity (Figures 4a, S3, and S4) suggests that trap states are also formed and unformed reversibly with temperature. We cannot define from our measurements the chemical nature of such trap states, but trapping at the strained epitaxial interface or the surface of the NR are likely candidates that are also consistent with thermal reversibility. The experiments presented in this work cannot distinguish between electron or hole trapping in an unambiguous manner. Although hole trapping has been identified in similar CdSe/CdS heterostructures,[38] evidence from transient absorption spectroscopy,[35,36,39] terahertz spectroscopy,[34] photoluminescence spectroscopy,[25,40] single NR spectroscopy,[37] cross-polarized grating spectroscopy,[41] multiexciton studies,[42] and Stark effect measurements[43] suggest that electron trapping is the more likely mechanism of temperature-dependent quenching, due to greater carrier delocalization to potential defect sites. The volume dependence of the

thermal stability of PL is a result of competition between thermally induced electron traps and radiative exciton recombination. For samples with a larger core volume fraction, exciton capture in the CdSe core is faster, evidenced by shorter PL lifetimes (Supporting Information Figure S7). Rapid radiative decay is more competitive with nonradiative processes that have increasing prominence at high temperature. Arrhenius plots of the nonradiative rate (Supporting Information Figure S8), estimated from $QY = k_{rad}/(k_{non\text{-}rad} + k_{rad})$, suggest a similar trap depth across the samples (~150−250 meV), bearing no clear relationship with the particle structures. This evidence suggests a common mechanism of carrier trapping across the samples, which is also similar to earlier reports.[2]

Figure 5e shows the results of these competing pathways for a series of dot-in-rod and one rod-in-rod sample. For consistency with the previous literature[40] and to avoid the ambiguity of multiexponential fitting,[44] we use empirical lifetimes defined as the time to decay to $I_0/3e^3$. In Figure 5e, we normalized the lifetime for each sample based on the lifetime taken at 300 K, in the solid state. Consistent with the steady-state PL data, the time-resolved PL shows different temperatures at which the decay time of dot-in-rod samples begins decreasing due to thermally induced nonradiative decay pathways. Each of the samples shows a region of increasing PL lifetime, but the peak PL decay temperature depends on the core volume fraction of the heterostructure. Starting with the same core material and growing increasingly longer NR shells, the largest CdSe/CdS dot-in-rod sample, with the smallest core volume fraction (3.5%), has a peak lifetime at 425 K; the second largest (4.9%) NR peaks at 450 K, and the smallest NR sample (10.8%) peaks at 500 K. The rod-in-rod heterostructure, in which the core NR comprises a much larger volume fraction of the total (16.3%), showed no maximum in the lifetime up to 600 K, as apparent in Figure 5c. Samples with longer radiative lifetimes at room temperature were ultimately less competitive with nonradiative relaxation and thus quenched more effectively at elevated temperature.

Earlier reports have suggested that the thermal decomposition of the ligand molecules on the particle surface dictates the stability of the NC PL at high temperatures.[1] We found that the oleic acid capped CdSe/CdS NCs that were also made by high-temperature seeded growth[28] performed similarly to phosphonate-capped NR heterostructures (Figure S4), indicating that at least among organic ligands the PL behavior is not affected by the ligand on the particles. However, we did not test an inorganic ligand, and we did not heat the samples above 600 K, situations in which it is possible that conclusions could be different. In one critical difference between the organic ligands, we found that oleate-capped core/shell NCs could not be redispersed after heating (insoluble or sparingly soluble in hexanes), evidence of ligand decomposition or reaction, whereas those with phosphonate ligands were readily soluble in hexanes after heating. This result likely reproduces the findings of an earlier report in which decomposition of carboxylate ligands is described as a possible cause of quenching. But we find no unambiguous evidence within our samples for distinctive temperature-dependent PL behavior in carboxylate- or phosphonate-capped NCs. We also note that the emission color of both sets of samples returned to the same energy (Figure S9), suggesting that no gross irreversible changes in the particle structure occurred.

Role of Nanocrystal Synthesis in the Thermal Stability of Photoluminescence. Different synthetic methods for preparing dot-in-rod and rod-in-rod NCs, which yield, to a first approximation, similar products, are clearly distinguished in temperature-dependent PL measurements. Early syntheses of monodisperse core/shell II−VI NCs frequently employed highly reactive metal chalcogenide precursors at lower concentration and lower temperature (*e.g.*, 120−200 °C) than the synthesis of the core particles.[45−50] Separately, seeded growth in CdSe/CdS heterostructures, in which NC seeds are injected at high temperature (>300 °C) into a reaction pot with low-reactivity precursors, has proven to be an effective method for synthesizing isotropic[28] and anisotropic[21−23] CdSe/CdS heterostructures. Both methods produce NCs with high room-temperature PL quantum yields and excellent color purity. We aimed as part of this work to test the relationship of synthetic conditions on the PL properties of samples under thermal stress.

The results already presented in this paper demonstrate the thermal PL properties from samples grown using seeded growth techniques. To provide samples for comparison with the samples of dot-in-rod and rod-in-rod samples shown above, we synthesized analogous heterostructures using dimethylcadmium and bis(TMS)sulfide as the Cd and S precursors in a coordinating mixture of hexadecylamine and trioctylphosphine oxide at 160−190 °C following literature protocols.[48−50] After precursor injection finished, the samples were annealed in solution at 100 °C for 2 h. Emission from the samples was quenched substantially more at elevated temperature than the samples synthesized by seeded growth, as shown in Figure 6a. Unlike the samples prepared by seeded growth, the CdSe/CdS dot-in-rod and rod-in-rod samples' lifetime data show a pattern similar to the properties of CdSe core-only samples, with decay time decreasing with higher temperature (Figure 6b and c).

Recent work on exceptionally bright core/shell quantum dots has suggested that formation of core/shell NCs at high temperature using low-reactivity precursors is instrumental in suppressing blinking and boosting quantum yields to near unity efficiency.[51] We speculate that high-temperature synthesis is instrumental in relaxing the NC structure and annealing samples to remove defect sites that could serve as

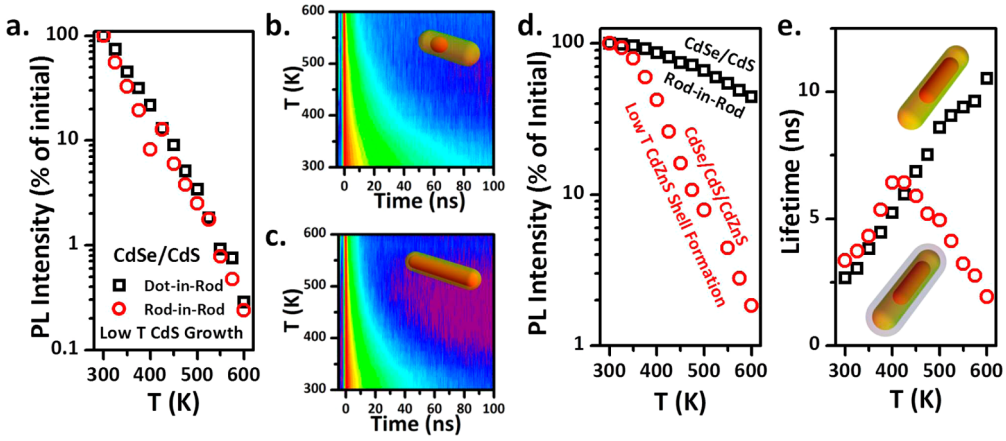

Figure 6. (a) Relative PL intensity of dot-in-rod and rod-in-rod NCs synthesized at low temperatures. The data are normalized to the intensity of the samples at 300 K. Time-resolved PL *versus* temperature contour plots for the same dot-in-rod (b) and rod-in-rod (c) samples analyzed in (a). Representative cartoons are inset. (d) Comparison of the preservation of PL in a sample of CdSe/CdS rods-in-rods as synthesized (black squares) and after additional shell growth with CdZnS at 190 °C (red circles). (e) Lifetime data collected as a function of temperature for the same samples in (d).

centers of nonradiative recombination. To extend this test, the best-performing rod-in-rod sample in this study was further overcoated at 190 °C with an alloyed CdZnS shell using literature procedures.[49] The thermal stability of emission of the samples is compared in Figure 6d. The CdSe/CdS/CdZnS double-shell NRs retained only a small fraction of their original PL intensity, more than a factor of 10 less than the CdSe/CdS rod-in-rod sample. The growth of an additional alloyed CdZnS shell at lower temperature substantially decreased thermal stability. The effective thermal annealing of samples in high-temperature syntheses ensures the formation of a shell with less susceptibility to thermal quenching, but the formation of a new shell introduces thermally susceptible material. Figure 6e shows that the lifetimes of the two samples diverge above 400 K, suggesting that defects in the CdZnS shell are the primary mechanism of quenching in the CdSe/CdS/CdZnS sample. Reversibility data showing irreversible loss of PL (Supporting Information Figure S10) show that the quenching process is likely due to permanent trap formation.

Temperature-Dependent Aniosotropy of CdSe/CdS Nanorods. Among the advantages of dot-in-rod or rod-in-rod samples for photonic applications is their high optical anisotropy, in the polarization of both emission and absorption.[23,52] Coupled to a programmable assembly, optical anisotropy offers a possibility of enhancing capture of emitted light through polarization-sensitive reflectance. Accurate measurement of optical anisotropy (R), which is defined by the ratio of intensities in eq 3,[44]

$$R = \frac{I_{\parallel} - I_{\perp}}{I_{\parallel} + 2I_{\perp}} \quad (3)$$

requires precise knowledge of the sample alignment. Solutions are the most reproducible way to generate isotropic alignments, and this strategy is used here, although the use of a commercial heating block limits this study to a maximum of 100 °C. Figure 7 shows the

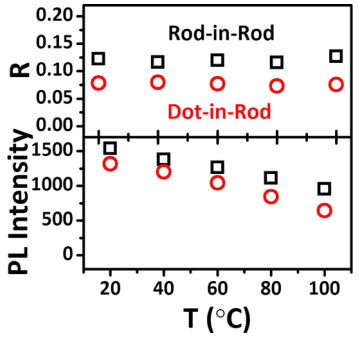

Figure 7. (a) Optical anisotropy (R) of CdSe/CdS rod-in-rod (black squares) and dot-in-rod (red circles) samples excited at 405 nm plotted *versus* temperature. (b) Integrated PL intensity of the same rod-in-rod (black squares) and dot-in-rod (red circles) samples plotted *versus* temperature.

temperature-dependent anisotropy (R) and fluorescence intensity for solutions of rod-in-rod and dot-in-rod samples dissolved in *n*-decane. Capped cuvettes and a high-boiling solvent were used to limit solvent evaporation at higher temperature and maintain a fixed concentration of NCs. Although the PL in solution drops, in a similar manner to the data collected in the solid state, the optical anisotropy of both samples remains fixed. This indicates that the electronic transitions responsible for absorption and emission remain the same despite the loss of PL. Temperature-dependent changes in the solvent viscosity of about 50%[53] might be expected to reduce the value of R through rotational depolarization,[44] but this effect is small. For NRs of this size, rotational depolarization occurs on the microsecond time scale[54] and photon emission occurs with nanosecond lifetimes, making the orientation of the emitting population nearly identical to that of the absorbing population.

CONCLUSIONS

The thermal stability of PL from CdSe/CdS nanoheterostructures has been studied as a function of

synthetically controllable dimensional and structural parameters using both steady-state and time-resolved spectroscopy. We have shown that the temperature-dependent behavior of samples prepared by seeded growth is similar to bulk CdSe, but that PL quenching is strongly determined by the core/shell volume ratio and the method of synthesis. Temperature-dependent time-resolved PL shows clear differences in the thermal behavior of samples consistent with the degree of preserved PL. We have also examined the influence of synthetic methods, specifically the preparation of the core/shell heterostructure, and found that the method for preparing the heteroepitaxial shell is very significant for determining thermal stability within the CdSe/CdS structures analyzed. Lastly, we performed temperature-dependent measurements of anisotropy and found that the samples show optical anisotropy that is temperature independent over the range measured.

EXPERIMENTAL METHODS

Syntheses and Structural Characterization. Synthesis of CdSe NCs,[22] CdSe/CdS dot-in-rod,[22,48] rod-in-rod,[23,49,50] and sphere-in-sphere[28] samples followed literature procedures. Transmission electron microscopy was performed using a JEOL 2100 microscope operated at 200 keV. X-ray diffraction measurements were performed on solutions in capillaries using a Rigaku Smartlab diffractometer.

Optical Spectroscopy. Routine solution-phase absorption and emission spectra were performed using a Cary 5000 UV–vis–NIR spectrometer and a Jobin-Yvonne Fluorolog-3 fluorimeter, respectively. For time-resolved PL data, a PicoQuant 405 nm diode was used at 1 MHz. Characterization of temperature-dependent PL was performed in an evacuated cell equipped with transparent windows (MMR R2300) with the heating stage controlled *via* an MMR K20 temperature controller. Samples were heated at 6 K/min and equilibrated 5 min for measurements. Temperature-dependent measurements in solution were performed using a Varian Eclipse fluorimeter equipped with a temperature-controlled sample holder. Hand-aligned polarizers were used for polarization-dependent measurements. Alignment was performed with a scattering sample (dried milk dispersed in water).

Conflict of Interest: The authors declare no competing financial interest.

Supporting Information Available: Additional electron microscopy, optical spectroscopy, sample data, and supporting theory can be found in the Supporting Information file. This material is available free of charge *via* the Internet at http://pubs.acs.org.

Acknowledgment. The authors thank Prof. Jeffery Saven for use of his instrumentation. This work was supported by the DOE, Office of Basic Energy Sciences, Division of Materials Science Award No. De-SC0002158. C.B.M. gratefully acknowledges the Richard Perry University Professorship.

REFERENCES AND NOTES

1. Rowland, C. E.; Liu, W.; Hannah, D. C.; Chan, M. K. Y.; Talapin, D. V.; Schaller, R. D. Thermal Stability of Colloidal InP Nanocrystals: Small Inorganic Ligands Boost High-Temperature Photoluminescence. *ACS Nano* **2013**, *8*, 977–985.
2. Rowland, C. E.; Schaller, R. D. Exciton Fate in Semiconductor Nanocrystals at Elevated Temperatures: Hole Trapping Outcompetes Exciton Deactivation. *J. Phys. Chem. C* **2013**, *117*, 17337–17343.
3. Yu, H. C. Y.; Leon-Saval, S. G.; Argyros, A.; Barton, G. W. Temperature Effects on Emission of Quantum Dots Embedded in Polymethylmethacrylate. *Appl. Opt.* **2010**, *49*, 2749–2752.
4. Zhao, Y.; Riemersma, C.; Pietra, F.; Koole, R.; de Mello Donegá, C.; Meijerink, A. High-Temperature Luminescence Quenching of Colloidal Quantum Dots. *ACS Nano* **2012**, *6*, 9058–9067.
5. Narayanaswamy, A.; Feiner, L. F.; Meijerink, A.; van der Zaag, P. J. The Effect of Temperature and Dot Size on the Spectral Properties of Colloidal InP/ZnS Core-Shell Quantum Dots. *ACS Nano* **2009**, *3*, 2539–2546.
6. Cheng, C.; Yan, H. Bandgap of the Core–Shell CdSe/ZnS Nanocrystal within the Temperature Range 300–373K. *Phys. E* **2009**, *41*, 828–832.
7. Dai, Q.; Song, Y.; Li, D.; Chen, H.; Kan, S.; Zou, B.; Wang, Y.; Deng, Y.; Hou, Y.; Yu, S.; *et al*. Temperature Dependence of Band Gap in CdSe Nanocrystals. *Chem. Phys. Lett.* **2007**, *439*, 65–68.
8. Valerini, D.; Cretí, A.; Lomascolo, M.; Manna, L.; Cingolani, R.; Anni, M. Temperature Dependence of the Photoluminescence Properties of Colloidal CdSe/ZnS Core/Shell Quantum Dots Embedded in a Polystyrene Matrix. *Phys. Rev. B* **2005**, *71*, 235409.
9. Jing, P.; Zheng, J.; Ikezawa, M.; Liu, X.; Lv, S.; Kong, X.; Zhao, J.; Masumoto, Y. Temperature-Dependent Photoluminescence of CdSe-Core CdS/CdZnS/ZnS-Multishell Quantum Dots. *J. Phys. Chem. C* **2009**, *113*, 13545–13550.
10. Narayanaswamy, A.; Feiner, L. F.; van der Zaag, P. J. Temperature Dependence of the Photoluminescence of InP/ZnS Quantum Dots. *J. Phys. Chem. C* **2008**, *112*, 6775–6780.
11. Gur, I.; Fromer, N. A.; Geier, M. L.; Alivisatos, A. P. Air-Stable All-Inorganic Nanocrystal Solar Cells Processed from Solution. *Science* **2005**, *310*, 462–465.
12. Kramer, I. J.; Sargent, E. H. The Architecture of Colloidal Quantum Dot Solar Cells: Materials to Devices. *Chem. Rev.* **2014**, *114*, 863–882.
13. Hikmet, R. A. M.; Chin, P. T. K.; Talapin, D. V.; Weller, H. Polarized-Light-Emitting Quantum-Rod Diodes. *Adv. Mater.* **2005**, *17*, 1436–1439.
14. Tessler, N.; Medvedev, V.; Kazes, M.; Kan, S.; Banin, U. Efficient Near-Infrared Polymer Nanocrystal Light-Emitting Diodes. *Science* **2002**, *295*, 1506–1508.
15. Kim, T.-H.; Cho, K.-S.; Lee, E. K.; Lee, S. J.; Chae, J.; Kim, J. W.; Kim, D. H.; Kwon, J.-Y.; Amaratunga, G.; Lee, S. Y.; *et al*. Full-Colour Quantum Dot Displays Fabricated by Transfer Printing. *Nat. Photonics* **2011**, *5*, 176–182.
16. Barnham, K.; Marques, J. L.; Hassard, J.; O'Brien, P. Quantum-Dot Concentrator and Thermodynamic Model for the Global Redshift. *Appl. Phys. Lett.* **2000**, *76*, 1197–1199.
17. Bronstein, N. D.; Li, L.; Xu, L.; Yao, Y.; Ferry, V. E.; Alivisatos, A. P.; Nuzzo, R. G. Luminescent Solar Concentration with Semiconductor Nanorods and Transfer-Printed Micro-Silicon Solar Cells. *ACS Nano* **2013**, *8*, 44–53.
18. Dang, C.; Lee, J.; Breen, C.; Steckel, J. S.; Coe-Sullivan, S.; Nurmikko, A. Red, Green and Blue Lasing Enabled by Single-Exciton Gain in Colloidal Quantum Dot Films. *Nat. Nanotechnol.* **2012**, *7*, 335–339.
19. Norris, D.; Bawendi, M. Measurement and Assignment of the Size-Dependent Optical Spectrum in CdSe Quantum Dots. *Phys. Rev. B* **1996**, *53*, 16338–16346.
20. Norris, D.; Efros, A.; Rosen, M.; Bawendi, M. Size Dependence of Exciton Fine Structure in CdSe Quantum Dots. *Phys. Rev. B* **1996**, *53*, 16347–16354.
21. Talapin, D. V.; Nelson, J. H.; Shevchenko, E. V.; Aloni, S.; Sadtler, B.; Alivisatos, A. P. Seeded Growth of Highly Luminescent CdSe/CdS Nanoheterostructures with Rod and Tetrapod Morphologies. *Nano Lett.* **2007**, *7*, 2951–2959.
22. Carbone, L.; Nobile, C.; De Giorgi, M.; Sala, F.; Della Morello, G.; Pompa, P.; Hytch, M.; Snoeck, E.; Fiore, A.; Franchini, I. R.; *et al*. Synthesis and Micrometer-Scale Assembly of Colloidal CdSe/CdS Nanorods Prepared by a Seeded Growth Approach. *Nano Lett.* **2007**, *7*, 2942–2950.

23. Sitt, A.; Salant, A.; Menagen, G.; Banin, U. Highly Emissive Nano Rod-in-Rod Heterostructures with Strong Linear Polarization. *Nano Lett.* **2011**, *11*, 2054–2060.
24. Van Embden, J.; Jasieniak, J.; Mulvaney, P. Mapping the Optical Properties of CdSe/CdS Heterostructure Nanocrystals: The Effects of Core Size and Shell Thickness. *J. Am. Chem. Soc.* **2009**, *131*, 14299–14309.
25. Rainò, G.; Stöferle, T.; Moreels, I.; Gomes, R.; Kamal, J. S.; Hens, Z.; Mahrt, R. F. Probing the Wave Function Delocalization in CdSe/CdS Dot-in-Rod Nanocrystals by Time- and Temperature-Resolved Spectroscopy. *ACS Nano* **2011**, *5*, 4031–4036.
26. Varshni, Y. P. Temperature Dependence of the Energy Gap in Semiconductors. *Physica* **1967**, *34*, 149–154.
27. Pisanello, F.; Leménager, G.; Martiradonna, L.; Carbone, L.; Vezzoli, S.; Desfonds, P.; Cozzoli, P. D.; Hermier, J.-P.; Giacobino, E.; Cingolani, R.; *et al.* Non-Blinking Single-Photon Generation with Anisotropic Colloidal Nanocrystals: Towards Room-Temperature, Efficient, Colloidal Quantum Sources. *Adv. Mater.* **2013**, *25*, 1973–1973.
28. Cirillo, M.; Aubert, T.; Gomes, R.; Van Deun, R.; Emplit, P.; Biermann, A.; Lange, H.; Thomsen, C.; Brainis, E.; Hens, Z. "Flash" Synthesis of CdSe/CdS Core−Shell Quantum Dots. *Chem. Mater.* **2014**, *26*, 1154–1160.
29. Pang, L.; Shen, Y.; Tetz, K.; Fainman, Y. PMMA Quantum Dots Composites Fabricated *via* Use of Pre-polymerization. *Opt. Express* **2005**, *13*, 44–49.
30. Jones, M.; Nedeljkovic, J.; Ellingson, R. J.; Nozik, A. J.; Rumbles, G. Photoenhancement of Luminescence in Colloidal CdSe Quantum Dot Solutions. *J. Phys. Chem. B* **2003**, *107*, 11346–11352.
31. Lee, J.-S.; Kovalenko, M. V.; Huang, J.; Chung, D. S.; Talapin, D. V. Band-like Transport, High Electron Mobility and High Photoconductivity in All-Inorganic Nanocrystal Arrays. *Nat. Nanotechnol.* **2011**, *6*, 348–352.
32. Tice, D. B.; Frederick, M. T.; Chang, R. P. H.; Weiss, E. A. Electron Migration Limits the Rate of Photobrightening in Thin Films of CdSe Quantum Dots in a Dry N_2 (g) Atmosphere. *J. Phys. Chem. C* **2011**, *115*, 3654–3662.
33. Labeau, O.; Tamarat, P.; Lounis, B. Temperature Dependence of the Luminescence Lifetime of Single CdSe/ZnS Quantum Dots. *Phys. Rev. Lett.* **2003**, *90*, 257404.
34. Kunneman, L. T.; Zanella, M.; Manna, L.; Siebbeles, L. D. A.; Schins, J. M. Mobility and Spatial Distribution of Photoexcited Electrons in CdSe/CdS Nanorods. *J. Phys. Chem. C* **2013**, *117*, 3146–3151.
35. Lupo, M. G.; Della Sala, F.; Carbone, L.; Zavelani-Rossi, M.; Fiore, A.; Lüer, L.; Polli, D.; Cingolani, R.; Manna, L.; Lanzani, G. Ultrafast Electron-Hole Dynamics in Core/Shell CdSe/CdS Dot/Rod Nanocrystals. *Nano Lett.* **2008**, *8*, 4582–4587.
36. De Vittorio, M.; Gil, B.; Kavokin, A.; Lupo, M. G.; Zavelani-Rossi, M.; Fiore, A.; Polli, D.; Carbone, L.; Cingolani, R.; Manna, L.; *et al.* Evidence of Electron Wave Function Delocalization in CdSe/CdS Asymmetric Nanocrystals. *Superlattices Microstruct.* **2010**, *47*, 170–173.
37. Rabouw, F. T.; Lunnemann, P.; van Dijk-Moes, R. J. A.; Frimmer, M.; Pietra, F.; Koenderink, A. F.; Vanmaekelbergh, D. Reduced Auger Recombination in Single CdSe/CdS Nanorods by One-Dimensional Electron Delocalization. *Nano Lett.* **2013**, *13*, 4884–4892.
38. Wu, K.; Rodríguez-Córdoba, W. E.; Liu, Z.; Zhu, H.; Lian, T. Beyond Band Alignment: Hole Localization Driven Formation of Three Spatially Separated Long-Lived Exciton States in CdSe/CdS Nanorods. *ACS Nano* **2013**, *7*, 7173–7185.
39. Grazia Lupo, M.; Scotognella, F.; Zavelani-Rossi, M.; Lanzani, G.; Manna, L.; Tassone, F. Band-Edge Ultrafast Pump−Probe Spectroscopy of Core/Shell CdSe/CdS Rods: Assessing Electron Delocalization by Effective Mass Calculations. *Phys. Chem. Chem. Phys.* **2012**, *14*, 7420–7426.
40. She, C.; Demortière, A.; Shevchenko, E. V.; Pelton, M. Using Shape to Control Photoluminescence from CdSe/CdS Core/Shell Nanorods. *J. Phys. Chem. Lett.* **2011**, *2*, 1469–1475.
41. Smith, E. R.; Luther, J. M.; Johnson, J. C. Ultrafast Electronic Delocalization in CdSe/CdS Quantum Rod Heterostructures. *Nano Lett.* **2011**, *11*, 4923–4931.
42. Sitt, A.; Della Sala, F.; Menagen, G.; Banin, U. Multiexciton Engineering in Seeded Core/Shell Nanorods: Transfer from Type-I to Quasi-Type-II Regimes. *Nano Lett.* **2009**, *9*, 3470–3476.
43. Müller, J.; Lupton, J. M.; Lagoudakis, P. G.; Schindler, F.; Koeppe, R.; Rogach, A. L.; Feldmann, J.; Talapin, D. V.; Weller, H. Wave Function Engineering in Elongated Semiconductor Nanocrystals with Heterogeneous Carrier Confinement. *Nano Lett.* **2005**, *5*, 2044–2049.
44. Lakowicz, J. *Principles of Fluorescence Spectroscopy*, 2nd ed.; Springer: New York, 2004; pp 291−319.
45. Hines, M. A.; Guyot-Sionnest, P. Synthesis and Characterization of Strongly Luminescing ZnS-Capped CdSe Nanocrystals. *J. Phys. Chem.* **1996**, *100*, 468–471.
46. Dabbousi, B. O.; Rodriguez-Viejo, J.; Mikulec, F. V.; Heine, J. R.; Mattoussi, H.; Ober, R.; Jensen, K. F.; Bawendi, M. G. (CdSe)ZnS Core−Shell Quantum Dots: Synthesis and Characterization of a Size Series of Highly Luminescent Nanocrystallites. *J. Phys. Chem. B* **1997**, *101*, 9463–9475.
47. Peng, X.; Schlamp, M. C.; Kadavanich, A. V.; Alivisatos, A. P. Epitaxial Growth of Highly Luminescent CdSe/CdS Core/Shell Nanocrystals with Photostability and Electronic Accessibility. *J. Am. Chem. Soc.* **1997**, *119*, 7019–7029.
48. Talapin, D. V.; Koeppe, R.; Götzinger, S.; Kornowski, A.; Lupton, J. M.; Rogach, A. L.; Benson, O.; Feldmann, J.; Weller, H. Highly Emissive Colloidal CdSe/CdS Heterostructures of Mixed Dimensionality. *Nano Lett.* **2003**, *3*, 1677–1681.
49. Deka, S.; Quarta, A.; Lupo, M. G.; Falqui, A.; Boninelli, S.; Giannini, C.; Morello, G.; De Giorgi, M.; Lanzani, G.; Spinella, C.; *et al.* CdSe/CdS/ZnS Double Shell Nanorods with High Photoluminescence Efficiency and Their Exploitation as Biolabeling Probes. *J. Am. Chem. Soc.* **2009**, *131*, 2948–2958.
50. Mokari, T.; Banin, U. Synthesis and Properties of CdSe/ZnS Core/Shell Nanorods. *Chem. Mater.* **2003**, *15*, 3955–3960.
51. Chen, O.; Zhao, J.; Chauhan, V. P.; Cui, J.; Wong, C.; Harris, D. K.; Wei, H.; Han, H.-S.; Fukumura, D.; Jain, R. K.; *et al.* Compact High-Quality CdSe-CdS Core-Shell Nanocrystals with Narrow Emission Linewidths and Suppressed Blinking. *Nat. Mater.* **2013**, *12*, 445–451.
52. Hadar, I.; Hitin, G. B.; Sitt, A.; Faust, A.; Banin, U. Polarization Properties of Semiconductor Nanorod Heterostructures: From Single Particles to the Ensemble. *J. Phys. Chem. Lett.* **2013**, *4*, 502–507.
53. Lee, A. L.; Ellington, R. T. Viscosity of n-Decane in the Liquid Phase. *J. Chem. Eng. Data* **1965**, *10*, 346–348.
54. Kamal, J.; Gomes, R.; Hens, Z.; Karvar, M.; Neyts, K.; Compernolle, S.; Vanhaecke, F. Direct Determination of Absorption Anisotropy in Colloidal Quantum Rods. *Phys. Rev. B* **2012**, *85*, 035126–1−035126−7.